Soil Biology and Biochemistry 198 (2024) 109544

Contents lists available at ScienceDirect

Soil Biology and Biochemistry

journal homepage: www.elsevier.com/locate/soilbio

Soil aggregate size distribution mediates microbial responses to prolonged acid deposition in a subtropical forest in south China

Jianping Wu [a,b,1], Xin Xiong [b,c,1], Dafeng Hui [d], Huiling Zhang [b,e], Jianling Li [b], Zhongbing Chang [f], Shuo Zhang [g], Yongxian Su [a], Xueyan Li [a], Deqiang Zhang [b,**], Qi Deng [b,*]

[a] Guangdong Provincial Key Lab of Remote Sensing and Geographical Information System, Guangdong Open Laboratory of Geospatial Information Technology and Application, Guangzhou Institute of Geography, Guangdong Academy of Sciences, Guangzhou, Guangdong, 510070, China
[b] Key Laboratory of Vegetation Restoration and Management of Degraded Ecosystems, South China Botanical Garden, Chinese Academy of Sciences, Guangzhou, Guangdong, 510650, China
[c] Jiangxi Provincial Key Laboratory of Carbon Neutrality and Ecosystem Carbon Sink, Lushan Botanical Garden, Jiangxi Province and Chinese Academy of Sciences, Jiujiang 332900, China
[d] Department of Biological Sciences, Tennessee State University, Nashville, TN, 37209, USA
[e] College of Biological & Pharmaceutical Sciences, China Three Gorges University, Yichang, 443002, China
[f] Key Laboratory of Natural Resources Monitoring in Tropical and Subtropical Area of South China, Surveying and Mapping Institute Lands and Resource Department of Guangdong Province, Guangzhou, Guangdong, 510670, China
[g] Forestry Policy Research Office of Zhaoqing High level Talent Training and Development Center, Municipal Bureau of Forestry, Zhaoqing, 526040, China

ARTICLE INFO

Keywords:
Acid rain
Soil aggregates
Soil microbial community
Soil enzyme activity
SOC stabilization and accumulation

ABSTRACT

Extended exposure to acid rain has vastly limited soil microbial activity with the consequences for soil carbon (C) storage, but less is known about the microbial responses within soil aggregates that to some extent determine soil C stabilization. Here, we investigated the main microbial group compositions and the relevant potential enzyme activities within different soil aggregates sizes (microaggregates (<250 μm), small macroaggregates (250–2000 μm), and microaggregates (>2000 μm)) in a subtropical forest with decade-long simulated acid rain (SAR) treatments. Four SAR treatments were set by irrigating plots with water of different pH values (i.e., 3.0, 3.5, 4.0, and 4.5 as a control). Results showed that the SAR treatment significantly inhibited microbial activities, specifically decreasing both bacterial and fungal abundances, leading to declines in C-degrading potential enzyme activities. Conversely, potential enzyme activities related to phosphorus (P) and nitrogen (N) mineralization as well as the enzyme stoichiometry for P/N ratio significantly increased under the SAR treatment. The SAR treatment showed no significant differences in microbial abundance across the three soil aggregate sizes. However, it had a more pronounced effect on potential enzyme activities in their optimal aggregate sizes, such as hydrolytic enzymes like β-glucosidase in macroaggregates and oxidases like phenol oxidase and peroxidase in microaggregates. Overall, C-degrading potential enzyme activities were more strongly decreased in the microaggregates than in macroaggregates, and the distribution in aggregates was significantly altered, transforming from large to small sizes under the SAR treatment, which together may boost SOC stabilization and accumulation. Additionally, our findings indicate that prolonged acid rain also caused soil nutrient limitation and imbalance, particularly for P, in subtropical forests. This study highlights the importance of soil aggregate size in regulating microbial responses to acid rain, which should be integrated into ecosystem models to predict soil biogeochemical cycles under future climate conditions.

1. Introduction

Due to escalating anthropogenic activities in recent decades, certain regions, particularly those in developing countries, have faced severe environmental pollution such as acid rain (Chen et al., 2021; Liu et al., 2021). In China, approximately 40% of the land area is affected by acid

* Corresponding author. South China Botanical Garden, Chinese Academy of Science 723 Xingke Road, Tianhe District, Guangzhou, Guangdong, 510650, China.
** Corresponding author.
E-mail addresses: wujianping@gdas.ac.cn (J. Wu), dengqi@scbg.ac.cn (Q. Deng).
[1] Co-first author.

https://doi.org/10.1016/j.soilbio.2024.109544
Received 9 May 2024; Received in revised form 29 July 2024; Accepted 3 August 2024
Available online 5 August 2024

rain, with the southern regions experiencing the most severe conditions, where pH levels often drop below 4 (Du et al., 2015; Liu et al., 2018). Despite longstanding emissions reduction policies implemented by the Chinese government, acid rain remains a persistent environmental challenge, primarily due to the rapid industrial expansion and an increase in motor vehicles use (Zeng et al., 2019). Previous researches have shown that prolonged exposure to acid rain further aggravates soil acidification, ultimately inhibiting microbial activity and altering soil biogeochemical cycles (Du et al., 2015; Meng et al., 2019; Liu et al., 2022). However, the extent to which acid rain affects soil carbon (C) storage and the underlying microbial mechanisms involved remains poorly understood (Averill and Waring, 2018).

Soil microorganisms play a pivotal role in C cycling and ecosystem health, contributing both through direct involvement in soil C decomposition and indirectly by influencing nutrient availability (Tian et al., 2019; Cheng et al., 2020). Research has shown that soil microbial communities are highly sensitive to acid rain and shifts in pH, although these findings are still debated (Zhalnina et al., 2015; Li et al., 2021a). For example, Rousk et al. (2009) discovered that all microbial variables were universally inhibited at pH levels below 4.5. Conversely, studies like Wang et al. (2018) have identified specific bacterial groups that thrive under acidic conditions. Moreover, changes in microbial community composition due to acid rain can affect enzyme activities, potentially impacting soil C concentration and nutrient availability (Sinsabaugh et al., 2009; Chen et al., 2022). Utilizing the dihydroxy phenylalanine (DOPA) assay, Sinsabaugh et al. (2008) observed a significant increase in phenol oxidase and peroxidase activities across 35 soils as pH decreased. Additionally, in latosol soil, Ling et al. (2010) reported increases in catalase and acid phosphatase activities in response to simulated acid rain. In contrast, Wang et al. (2010) found that simulated acid rain reduced the activities of cellulose, acid phosphatase, and polyphenol oxidase, but increased the catalase activities. Consequently, gaining a better understanding of microbial response to acid rain is essential for predicting soil C cycling within ecosystem.

Soil C accumulation and stabilization, to some extent, contingent upon soil aggregate structures, which can be categorized into three categories based on diameter: large macroaggregates (>2000 μm), small macroaggregates (250–2000 μm), and microaggregates (<250 μm) (Fang et al., 2016; Ozlu and Arriaga, 2021). Generally, macroaggregates contain relatively active and unstable C from recent inputs of plant residue and fungal mycelium (Six et al., 2004; Awad et al., 2018), whereas microaggregates are primarily composed of primary particles bonded with polyvalent metal cations and polysaccharide polymers, humus, or organic debris, which better protect C from microbial degradation (Dorodnikov et al., 2009). Thus, the soil C turnover rate typically decreases with smaller aggregate sizes (Tian and Niu, 2015). Soil aggregate structures also create spatial heterogeneity for microorganisms by offering diverse ecological niches with varied physicochemical characteristics (Chen et al., 2015; Wang et al., 2017). Bacterial groups often occupy the small pore spaces within microaggregates to evade predators like protozoa (Jastrow et al., 2007; Rabbi et al., 2016), while fungi preferentially proliferate in the larger pore spaces within macroaggregates, which are favorable for fungal mycelium spread (Garcia-Franco et al., 2015). In addition, microorganisms contribute to biogeochemical cycling primarily through the production of specialized extracellular enzymes (Luo et al., 2017; Nannipieri et al., 2018). For example, C-degrading enzymes are essential for SOC cycling by breaking down complex organic compounds into simple molecules that microbes can assimilate. These enzyme activities indicate the type and distribution of organic materials within soil aggregates. Hydrolytic enzymes, such as *β*-glucosidase (BG) and cellobiohydrolase (CBH), are crucial for breaking down cellulose and hemicellulose in plant residues, which are more abundant in macroaggregates. Oxidases like phenol oxidase (PhOx) and peroxidase (Perox), decompose lignin and other complex organic compounds, contributing to SOC stabilization within microaggregates and mineral-associated organic matter (Waring et al., 2014). Changes in microbial community composition across different soil aggregates can influence enzyme activities (Sinsabaugh et al., 2009; Yu et al., 2020), affecting C degradation within aggregates and, consequently, soil C storage (Nie et al., 2014; Lu et al., 2021). Although considerable attention has been paid to the structure of soil aggregates and the microbial heterogeneity within them, there remains limited understanding of how microbial response to the interaction between soil aggregates and acid rain might alter aggregate distribution and, in turn, impact SOC stabilization and accumulation.

Here, we conducted a decade-long in-situ experiment to investigate how simulated acid rain (SAR) affects microbial responses within aggregates of three different sizes and its consequential impact on soil organic carbon (SOC) concentration in a subtropical forest in southern China. Our previous works have demonstrated that the SAR treatment decreased soil respiration and increased SOC accumulation, and solid-state ^{13}C-NMR spectroscopy has revealed that SOC stabilization was enhanced under the SAR treatment (Wu et al., 2016, 2020; Chen et al., 2022). However, the degree of SOC stabilization is highly dependent on the structure of soil aggregates, alongside the microbial communities and the potential activities of microbial-derived enzymes within these aggregates. Therefore, we hypothesized that the SAR treatment would alter predominant microbial compositions and inhibit specific potential enzyme activities. These microbial responses are expected to vary across different aggregate sizes, potentially affecting the distribution of soil aggregates by size and, thus, impacting the SOC stabilization and accumulation.

2. Material and methods

2.1. Study site

This research was conducted within the Dinghushan National Nature Reserve, located in Guangdong Province, China, with coordinates spanning from 23°09′21″ to 23°11′30″N and 112°30′39″ to 112°33′41″E. This region experiences a typical subtropical humid monsoon climate, characterized by an average annual temperature of 22.3 °C and an average annual precipitation of 1927 mm. Our study site was established within a mature monsoon evergreen broadleaf forest, estimated to be over 400 years old. Dominant canopy species observed included *Schima superba*, *Cryptocarya concinna*, *Castanopsis chinensis*, *Syzygium rehderianum*, *Cryptocarya chinensis*, and *Machilus chinensis*. Over the past decades, this area has been significantly impacted by prevalent acid rain, resulting in an annual average pH below 4.50 (Lu et al., 2014).

2.2. Experimental design

This prolonged field experiment commenced in June 2009, with a detailed description of the experimental layout available in Liang et al. (2013) and Wu et al. (2016). Brief, the SAR treatment involved irrigation with water of three pH value levels: T1 (pH 4.0), T2 (pH 3.5), and T3 (pH 3.0). The control group (CK) utilized local lake water with a pH of approximately 4.5. Each treatment included three replicated plots, making a total 12 plots randomly distributed across the site. Each plot measured 10 m × 10 m and was separated from adjacent plots by a buffer zone of more than 3 m. To reflect the chemical composition of local acid deposition, a 1:1 M ratio of H_2SO_4 and HNO_3 was dissolved in local water to prepare the acidic solution for each treatment. The SAR solutions were applied to each plot below the canopy using a gasoline engine sprayer, and the amount applied to each plot was 40 L per application. Each plot was sprayed twice a month during the experimental period. During the application, the H^+ added to each plot was 9.6, 32, 96 mol $ha^{-1}yr^{-1}$ in the T1, T2, T3 treatments, respectively, which was equal to about 0.6, 2.0 and 6.0 times of that in the through-fall of the forest.

2.3. Sample collection and aggregate fractionation

In September 2020, soil samples were gathered from the topsoil layer (0–10 cm) in each plot by taking 10 random soil cores after clearing away any stones and litter. These collected samples underwent a two-fold division for further analysis. One portion of the fresh soil samples was preserved at 4 °C, primed for detailed soil aggregate fractionation and microbial analysis, while the other portion was allowed to air-dry and subsequently used for analyzing soil properties.

To maintain the soil aggregates' bioactivity and minimize disruption, we implemented an optimized dry-sieving method with an optimal moisture level ranging from 10% to 15%, drawing inspiration from the methodologies outlined by Dorodnikov et al. (2009) and Fang et al. (2016). The bulk soil samples that met the appropriate moisture condition were carefully sieved through an 8-mm sieve to eliminate visible plant residues and stones. For further fractionation, pre-treated soil samples weighing 500 g were subjected to a sequence of nested sieves with pore sizes of 2000 μm and 250 μm, and shaken at a rate of 100 rounds per minute for 2 min. This method effectively separated the soil aggregates into three distinct fractions: large macroaggregates (exceeding 2000 μm), small macroaggregates (ranging from 250 to 2000 μm), and microaggregates (less than 250 μm). Subsequently, a portion of the subsample was designated for biotic analysis, while another portion was allocated for abiotic analysis.

2.4. Analysis of microbial community composition

The composition of the soil microbial community was assessed using phospholipid fatty acid analysis (PLFA), following the method outlined by Bossio and Scow (1998). Fresh soil samples underwent freeze-drying before extraction, fractionation, and gas chromatography analysis. Specific PLFAs served to identify different microbial groups (Streit et al., 2014; Bai et al., 2017). Gram-positive (G^+) bacteria were distinguished by the presence of specific phospholipid fatty acids, including 15:0a, 15:0i, 16:0i, 17:0a, and 17:0i fatty acids, while Gram-negative (G^-) bacteria were characterized by 16:1ω7c, cyclic 17:0cy, 18:1ω7c, and cyclic 19:0cy. Actinomycetes were distinguished by PLFAs 10Me 16:0, 10Me 17:0 and 10Me 18:0. Total bacterial PLFAs were determined by the presence of biomarkers for G^+ bacteria, G^- bacteria, actinomycetes, as well as PLFAs 14:0, 15:0, 16:0 and 18:0. Similarly, total fungal PLFAs were assessed using PLFAs 18:1ω9c, 18:2ω6c and 18:3ω3c.

2.5. Analysis of potential enzyme activity

This study evaluated six soil potential enzyme activities (Table S1), encompassing four hydrolytic enzymes (acid phosphomonoesterase (AP), N-acetylglucosaminidase (NAG), β-glucosidase (BG), cellobiohydrolase (CBH)), along with two oxidases (phenol oxidase (PhOx), peroxidase (Perox)). While not entirely equivalent, these enzyme assays were chosen to represent key microbial processes involved in C and nutrient degradation within the soil, as highlighted in previous studies (e.g., Nie et al., 2014; Nannipieri et al., 2018; Zheng et al., 2022).

The measurement of potential BG, CBH, AP, and NAG activities employed a colorimetric assay as per Tabatabai (1994)'s method, which quantifies *p*-nitro-phenol release from specific synthetic substrate cleavage. To assess BG potential activity, a mixture containing 1.0 g of fresh soil samples were mixed, 4 mL of modified universal buffer at pH 6.0, and 1 mL of 0.025 M *p*-nitrophenyl-β-D-glucopyranoside was incubated at 37°C for an hour. The enzymatic reaction was then terminated by adding 0.1 M trihydroxymethyl aminomethane (pH 12) and 0.5 M $CaCl_2$. The filtered mixtures were subsequently analyzed for absorbance at 400 nm using a spectrophotometer (UV-1700, Shimadzu, Columbia, MD, USA) (Tabatabai, 1994; Fang et al., 2016). The assay procedures for potential AP, CBH, and NAG activities are consistent with those used for BG. However, specific synthetic substrates and optimal pH conditions are adjusted according to the enzyme type: AP assays use *p*-nitrophenylphosphate and buffer at pH 6.5, CBH use *p*-nitrophenyl-β-D-cellobioside with a pH of 5.0, and NAG employs *p*-nitrophenyl-N-acetyl-β-D-glucosaminidine at pH 5.5, respectively, following protocols established in the previous literatures (Tabatabai, 1994; Parham and Deng, 2000; Wang et al., 2015a).

To measure the potential activities of PhOx and Perox, we applied the protocol by Iyyemperumal and Shi (2008) with L-3, 4- dihydroxy phenylalanine (L-DOPA) as the substrate. For PhOx, 1 g of fresh soil sample was combined with 4.5 mL modified universal buffer at pH 5.0 and 0.01 M L-DOPA and incubated at 25 °C for an hour. Then centrifuged at 12,000 g for 5 min at 5 °C to stop the reaction. The clear supernatant was then filtered and analyzed for absorbance at 450 nm using a fluorescence spectrometer. For Perox, the procedure was identical except for an initial addition of 1 mL of 0.3% H_2O_2.

We quantified the relative acquisition of C versus nutrients, and the relative N versus P using potential enzyme activity measurements, following methodologies from Fanin et al. (2016) and Moorhead et al. (2016). The sum of potential BG, CBH, PhOx and Perox activities represented C acquisition, while N and P acquisition were represented by potential NAG and AP activities, respectively. We determined the enzyme stoichiometry for C: N, C: P and P: N using the potential enzyme activity ratios as (BG + CBH + PhOx + Perox)/(BG + CBH + Phox + Perox + NAG), (BG + CBH + PhOx + Perox)/(BG + CBH + PhOx + Perox + AP), and AP/(NAG + AP), respectively (Nie et al., 2014).

2.6. Soil chemical properties analyses

Soil pH was assessed by immersing a glass electrode into a mixture with a 1:2.5 soil-to-water ratio, following procedures from Dick et al. (2000). The concentration of SOC were measured using a potassium dichromate ($K_2Cr_2O_7$) wet digestion method as specified by Nelson and Sommers (1982). The fine root biomass (diameter ≤2 mm) in the 0–10 cm soil profile was sampled using a stainless-steel corer (6.8 cm interior diameter) and subsequently dried at 60 °C for 48 h and weighed. The soil readily oxidation organic carbon (ROC) concentration was measured by 333 Mm $KMnO_4$ oxidation following Blair et al. (1995). The non-readily oxidation organic carbon (NROC) concentration was calculated from difference between total SOC concentration and ROC concentration.

2.7. Statistical analysis

The effect of SAR treatment on the proportion of soil aggregates, fine root biomass, ROC and NROC concentrations were assessed using a one-way analysis of variance (ANOVA) with post-hoc LSD test for identifying significant differences. The combined effects of SAR treatment and soil aggregate sizes on soil pH value, SOC, TN, microbial community composition, and potential enzyme activities were analyzed via two-way ANOVA. We also utilized the Pearson correlation analysis to investigate the interrelations among soil properties, microbial parameters, and potential enzyme activities. All statistical SPSS software version 20.0 (SPSS, Inc., Chicago, IL, USA) was used for all statistical analyses, with significance determined at $P < 0.05$. Additionally, CANOCO software conducted redundancy analysis (RDA) to assess the interactions between soil microbial group abundance and potential enzyme activities across various soil aggregate sizes under the SAR treatment.

3. Results

3.1. Soil parameters and aggregates distribution

The SAR treatment notably lowered soil pH ($P < 0.05$), though no significant differences in soil pH were observed across the three different aggregate sizes. Notable interactive effects ($P < 0.05$) were observed between SAR treatment and aggregate size on the SOC concentration (Fig. 1a). The SOC concentration increased significantly under the SAR treatment, with more pronounced increases occurred in smaller

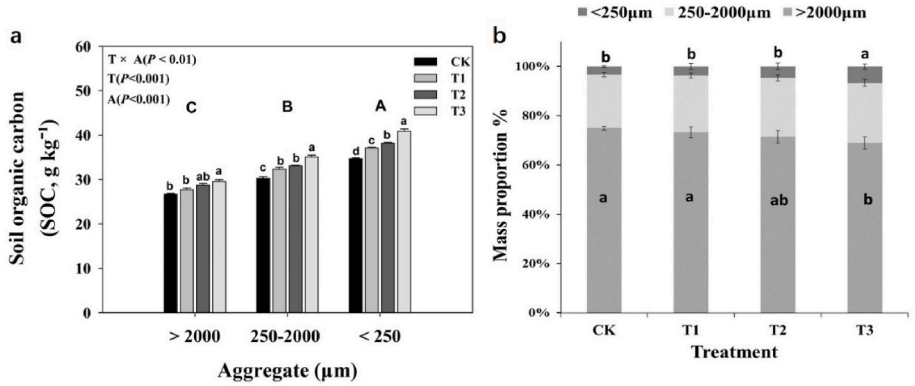

Fig. 1. Variation of soil organic carbon concentration (SOC, g kg^{-1}) among three soil aggregate sizes (a) and the mass proportions of different soil aggregates (b) under the SAR treatment. Statistical differences are denoted by superscript letters: uppercase for aggregate size classes and lowercase for SAR treatments. The values in parentheses are two-way ANOVA analyses (P values) on effects of the SAR treatments (T), aggregate size classes (A) and their interactions (T × A).
> 2000 μm, large macroaggregates; *250*-2000 μm, small macroaggregates; < 250 μm, microaggregates; *CK*, local lake water with a pH of approximately 4.5; *T1*, pH 4.0; *T2*, pH 3.5, and *T3*, pH 3.0.

aggregate sizes (Fig. 1a). In addition, the concentrations of ROC and NROC in the bulk soil did not show significant differences under the SAR treatment initially. However, as the SAR experiment progressed, both ROC and NROC concentrations increased significantly with decreasing pH (Fig. S1). We also found that the SAR treatment significantly decreased the fine root biomass, a proxy for plant root growth (Fig. S2).

In the control plots, the weight distribution in the large macroaggregates accounted for the majority of the bulk soil weight, ranging from 66% to 75%, significantly higher than the weight proportions in small macroaggregates (ranging from 21% to 29%) and microaggregates (ranging from 2% to 5%) (Fig. 1b). Weight distribution in soil aggregates was changed by the SAR treatment. In comparison to the control plots, the T3 treatment decreased in the proportion of large macroaggregates from 75% to 69%. Conversely, the proportion of small macroaggregates increased from 22% to 27%, and the proportion of microaggregates increased from 3% to 4% (Fig. 1b). However, no significant differences were observed in the proportions of large macroaggregates and small macroaggregates between the T1, T2, and CK treatments, nor between T2 and T3 treatments.

3.2. Soil microbial community composition

The concentration of total microbial PLFAs was significantly higher in small macroaggregates compared to both large macroaggregates and microaggregates. Total bacterial and fungal PLFAs accounted for 80.1–86.7% and 7.5–9.2% of total microbial PLFAs, respectively, with significantly differences among the aggregate sizes. Large macroaggregates exhibited significantly higher total bacterial PLFA concentrations than both small macroaggregates and microaggregates, whereas total fungal PLFAs were considerably lower in microaggregates than in macroaggregates. Small macroaggregates had the highest abundance of G^- bacteria compared to other sizes. Additionally, large macroaggregates had a significantly higher fungal to bacterial PLFAs ratio (F: B ratio), and the highest ratio of G^+ to G^- bacteria (G^+: G^- ratio) was

Table 1
Effects of simulated acid rain (SAR) treatment and soil aggregate size on soil pH, total nitrogen (TN, g kg^{-1}), phospholipids fatty acid (PLFAs) biomarkers content (nmol g^{-1} dry soil), and biomarker ratios.

		pH	TN	Total PLFAs	Bacteria	Fungi	G+ bacteria	G- bacteria	Actinomycetes	F: B ratio	G+: G- ratio
Aggregate (μm)	>2000	3.77 ± 0.02	2.03 ± 0.05B	19.28 ± 0.50B	16.72 ± 0.41A	1.78 ± 0.11A	4.14 ± 0.17	1.81 ± 0.07B	2.07 ± 0.08	0.11 ± 0.01A	2.29 ± 0.05B
	250–2000	3.77 ± 0.03	2.20 ± 0.05B	20.70 ± 0.48A	16.92 ± 0.34A	1.41 ± 0.04B	4.60 ± 0.19	2.07 ± 0.08A	2.38 ± 0.10	0.08 ± 0.01B	2.22 ± 0.04B
	<250	3.79 ± 0.02	2.47 ± 0.11A	18.46 ± 0.33B	14.79 ± 0.24B	1.39 ± 0.04B	4.13 ± 0.15	1.67 ± 0.05B	2.22 ± 0.06	0.09 ± 0.01B	2.47 ± 0.05A
Treatment	CK	3.86 ± 0.01a	2.19 ± 0.10	21.06 ± 0.59a	16.97 ± 0.56a	1.73 ± 0.10a	4.54 ± 0.25	1.92 ± 0.10	2.22 ± 0.13	0.11 ± 0.01A	2.36 ± 0.06
	T1	3.80 ± 0.02b	2.18 ± 0.08	19.64 ± 0.48b	16.44 ± 0.49 ab	1.59 ± 0.09 ab	4.06 ± 0.14	1.81 ± 0.09	2.18 ± 0.09	0.10 ± 0.01AB	2.26 ± 0.06
	T2	3.74 ± 0.04c	2.24 ± 0.12	19.17 ± 0.49BCE	16.01 ± 0.46 ab	1.41 ± 0.05b	4.47 ± 0.21	1.85 ± 0.11	2.30 ± 0.24	0.09 ± 0.01B	2.43 ± 0.08
	T3	3.70 ± 0.03d	2.31 ± 0.13	18.04 ± 0.34c	15.14 ± 0.38b	1.36 ± 0.10b	4.10 ± 0.19	1.81 ± 0.09	2.19 ± 0.09	0.09 ± 0.01B	2.26 ± 0.04
Analysis of variance (*P* values)											
Aggregate (A)		0.120	0.005	0.002	<0.001	<0.001	0.101	0.002	0.064	<0.001	0.002
Treatment (T)		<0.001	0.786	<0.001	0.007	0.001	0.207	0.755	0.809	0.036	0.056
A × T		0.171	0.958	0.393	0.567	0.300	0.585	0.446	0.724	0.294	0.370

Values are means ± SE. Different superscript letters indicate differences at a significance level of $P < 0.05$ (uppercase for aggregate size classes and lowercase for SAR treatments). > 2000 μm, large macroaggregates; *250*-2000 μm, small macroaggregates; < 250 μm, microaggregates; *CK*, local lake water with a pH of approximately 4.5; *T1*, pH 4.0 treatment; *T2*, pH 3.5 treatment; *T3*, pH 3.0 treatment; *Total PLFAs*, Total PLFA concentration; *G^+ bacteria*, Gram-positive bacteria; *G^- bacteria*, Gram-negative bacteria; *F: B ratio*, the ratio of fungal biomass to bacterial biomass; *G^+: G^- ratio*, the ratio of Gram-positive bacterial biomass to Gram-negative bacterial biomass.

observed in microaggregates (Table 1).

Our results indicated that the SAR treatment significantly affected the concentrations of total microbial, bacterial, and fungal PLFAs, as well as the F: B ratio ($P < 0.05$). For other microbial groups, no significant effect of the SAR treatment was found. Compared to the control, total microbial PLFAs decreased by 6.7% in the T1 treatment, 9.0% in the T2 treatment, and 14.3% in the T3 treatment, while total bacterial and fungal PLFAs in T3 treatment decreased by 10.8 and 21.4%, respectively (Table 1).

3.3. Soil potential enzyme activities

Results revealed a significant effect of aggregate size on almost all selected potential enzyme activities ($P < 0.05$, Fig. 2), except for the potential CBH activity. Potential BG activity was highest in large macroaggregates, exceeding those observed in small macroaggregates and microaggregates. The potential activities of two oxidases (PhOx and Perox) and AP were markedly higher in microaggregates compared to macroaggregates, whereas potential NAG activity was significantly lower in microaggregates relative to macroaggregates.

Significant interactive effects were observed between SAR treatment and aggregate size on the potential activities of BG, PhOx, Perox and AP ($P < 0.05$, Fig. 2). The SAR treatment led to a notable decrease in potential BG activity, particularly in larger aggregates ($P < 0.05$, Fig. 2). Additionally, the potential activities of PhOx and Perox were also decreased significantly under the SAR treatment, with a greater reduction observed in microaggregates than in macroaggregates. Conversely, potential AP activity experienced an increase under the SAR treatment, particularly in microaggregates compared to macroaggregates. While the SAR treatment, except for the T3 treatment, also had significant positive effects on the potential activities of CBH and NAG, but no significant interactive effect with aggregate size was observed.

3.4. Soil enzyme stoichiometry

Results demonstrated that enzyme stoichiometry was significantly influenced by aggregate sizes in our study ($P < 0.05$, Fig. 3). As aggregate size decreased, there was an increase in the total P: N enzyme activity ratio, while the total C: P enzyme activities ratio was lower in microaggregates compared to macroaggregates under the effect of SAR treatment (Fig. 3). Additionally, large macroaggregates exhibited a significantly lower total C: N enzyme activity ratio than both small macroaggregates and microaggregates.

The SAR treatment and aggregate size showed a significant interactive effect on C: P and P: N enzyme activity ratios ($P < 0.05$, Fig. 3). The C: P enzyme activity ratio was decreased under the SAR treatment, particularly in macroaggregates compared to microaggregates. Conversely, the P: N enzyme activity ratio increased, more pronounced in smaller aggregates. However, the C: N enzyme activity ratio showed no significant change under the SAR treatment across different

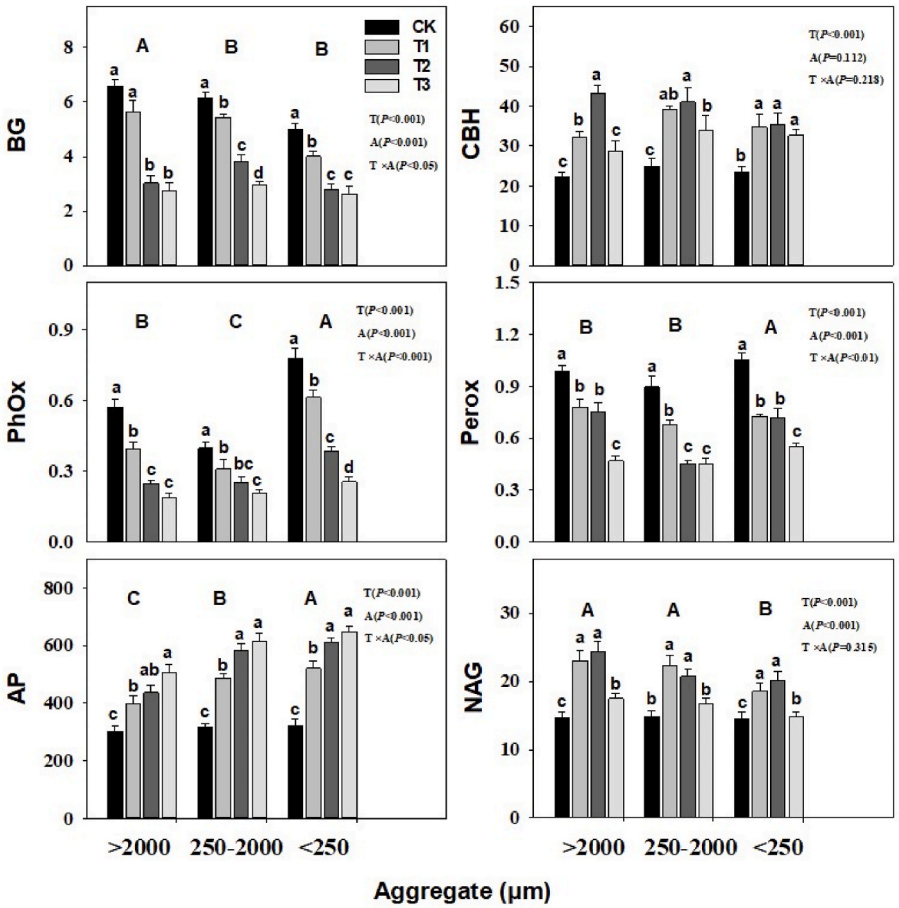

Fig. 2. Interactive effects between SAR treatment and aggregate size on the potential enzyme activities. Statistical differences are denoted by superscript letters: uppercase for aggregate size classes and lowercase for SAR treatments. The values in parentheses are two-way ANOVA analyses (*P* values) on effects of the SAR treatments (T), aggregate size classes (A) and their interactions (T × A).
BG, potential *β*-glucosidase activity; *CBH*, potential cellobiohydrolase activity; *PhOx*, potential phenol oxidase activity; *Perox*, potential peroxidase activity; *AP*, potential acid phosphomonoesterase activity; *NAG*, potential *N*-acetylglucosaminidase activity. > 2000 μm, large macroaggregates; *250*-2000 μm, small macroaggregates; < 250 μm, microaggregates. *CK*, local lake water with a pH of approximately 4.5; *T1*, pH 4.0; *T2*, pH 3.5, and *T3*, pH 3.0.

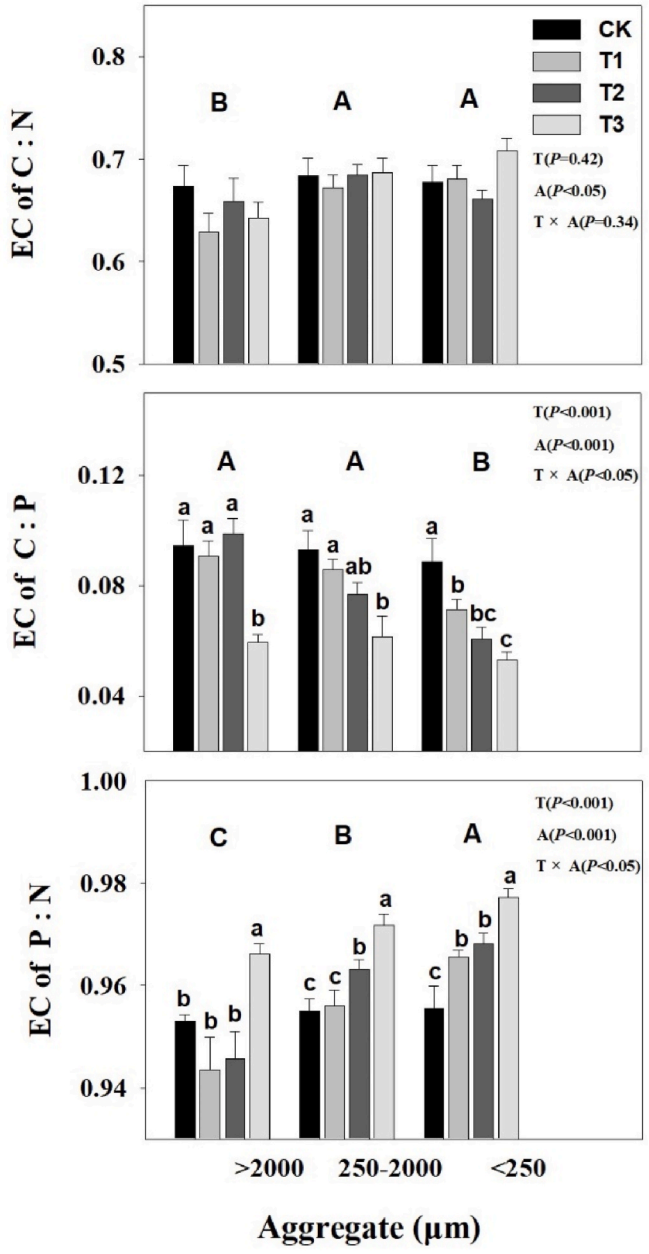

Fig. 3. Interactive effects between SAR treatment and aggregate size on the enzyme stoichiometry (EC). Statistical differences are denoted by superscript letters: uppercase for aggregate size classes and lowercase for SAR treatments. The values in parentheses are two-way ANOVA analyses (P values) on effects of the SAR treatments (T), aggregate size classes (A) and their interactions (T × A). > 2000 μm, large macroaggregates; *250*-2000 μm, small macroaggregates; < 250 μm, microaggregates. *CK*, local lake water with a pH of approximately 4.5; *T1*, pH 4.0; *T2*, pH 3.5, and *T3*, pH 3.0. ES of C: N, C: P and P: N were calculated as potential enzyme activities (BG + CBH + PhOx + Perox)/(BG + CBH + Phox + Perox + NAG), (BG + CBH + PhOx + Perox)/(BG + CBH + PhOx + Perox + AP) and AP/(NAG + AP), respectively.

aggregate sizes.

3.5. Correlations analyses among microbial response and soil parameters

According to Table 2, total microbial PLFAs in macroaggregates show a positive correlation with soil pH and the SOC concentration, which is not the case in microaggregates. Bacterial PLFAs in macroaggregates have a positive relationship with soil pH but a negative one with SOC concentration. Similarly, fungal PLFAs in microaggregate and small macroaggregates also exhibit positive correlations with soil pH and negative with SOC concentration. Only in microaggregates, G^- bacterial PLFAs and F: B ratio show positive correlations with soil pH (Table 2). Across all aggregate sizes, soil pH positively associated with the potential activities of BG, PhOx, Perox, and the enzyme stoichiometry for P/N ratio (Fig. 4). However, significantly quadratic relationships were found between soil pH and CBH activity in microaggregate, while with NAG activity in macroaggregates, respectively.

In macroaggregates, significant correlations were observed between total microbial PLFAs and most soil potential enzyme activities, except for CBH and NAG (Table 2). Potential PhOx and AP activities are significantly correlated with bacterial PLFAs, while potential Perox activity correlates significantly with bacterial PLFAs only in large macroaggregates. Conversely, potential activities of PhOx and AP exhibited significant positive correlation with fungal PLFAs in both large macroaggregates and microaggregates. In microaggregates specifically, both potential BG and Perox activities had a significant correlation with total fungal PLFAs. Furthermore, the F: B ratio in microaggregates significantly correlates with both potential PhOx and Perox activities. Additional redundancy analysis reveals that in macroaggregates, potential BG, PhOx and Perox activities were predominantly influenced by total bacterial PLFAs, while in microaggregate, they were mainly controlled by fungal PLFAs. In small macroaggregates, soil potential enzyme activities appear to be influenced by both bacterial and fungal PLFAs (Fig. 5).

4. Discussion

Our study provides further evidence that prolonged exposure to acid rain significantly increases SOC concentration, especially in smaller soil aggregates where its impact is more pronounced. This corroborates findings from our previous research at the same site, which reported increased SOC stabilization and accumulation using solid-state CP/MAS ^{13}C-NMR spectroscopy analysis (Wu et al., 2016). The observed increase in SOC concentration under the SAR treatment may be associated with reduced soil respiration, aligning with previous studies (Liang et al., 2013; Wu et al., 2016). The simultaneous increase in both ROC and NROC under high-intensity acid treatment might be a contributing factor to the observed increase in total SOC concentration (Fig. S1). Soil ROC, including labile organic carbon from plant litter, soil microfauna, and root exudates, tends to be readily utilized by microbes. However, reduced microbial and hydrolytic enzymes activities (e.g., BG), under acid rain conditions may have led to decreased utilization of these labile carbon sources, inhibiting the mineralization rate of soil organic carbon and reducing heterotrophic respiration. As a result, this portion of organic carbon was preserved rather than decomposed, leading to its accumulation. While this increase in ROC might reduce the overall stability of SOC due to its high decomposability, our results indicate that the content of ROC shows a tendency to decrease over time with continued acid rain exposure, even if this trend wasn't statistically significant annually. The NROC refers to the portion of SOC that is chemically stable and resistant to microbial decomposition. This fraction's accumulation may be attributed to the "preferential substrate utilization principle", where microbes prioritize the use of more labile carbon sources, thus reducing the utilization efficiency of the stable fraction. Additionally, acid rain was found to inhibit the activities of soil enzymes related to the decomposition of the stable fraction of SOC, such as PhOx and Perox, leading to an accumulation of this more recalcitrant carbon fraction. the increase in the stable fraction of SOC under these conditions not only supports the accumulation of total SOC but also enhances its stability, as the stable fraction is less susceptible to microbial decomposition.

Additionally, this reduction parallels a decrease in microbial abundance and the activity of C-degrading enzymes noted in this study, possibly driven by heightened toxicity from extractable aluminum

Table 2
Pearson correlation between soil pH, microbial variables, and soil enzyme stoichiometry among different soil aggregate sizes.

	pH	Total PLFAs	Bacteria	Fungi	G^+ bacteria	G^- bacteria	Actinomycetes	F: B ratio
Large macroaggregates								
pH	1	0.759[b]	0.681[a]	0.597	−0.133	−0.214	−0.263	0.385
SOC	−0.766[b]	−0.795[b]	−0.676[a]	−0.664	0.170	0.346	0.237	−0.516
BG	0.862[b]	0.616[a]	0.514	0.655[a]	−0.398	−0.227	−0.530	0.508
CBH	−0.240	−0.174	0.058	−0.254	0.279	0.109	0.392	−0.248
PhOx	0.883[b]	0.840[b]	0.736[b]	0.758[b]	−0.183	−0.139	−0.329	0.579
Perox	0.838[b]	0.711[b]	0.724[b]	0.419	−0.185	−0.362	−0.294	0.297
AP	−0.839[b]	−0.728[b]	−0.630[a]	−0.562	0.225	0.295	0.381	−0.521
NAG	−0.136	−0.32 4	0.185	−0.270	0.017	−0.098	0.131	−0.435
ES of C: N	0.051	0.314	0.026	0.134	0.221	0.194	0.185	0.422
ES of C: P	0.592[a]	0.586[a]	0.476	0.334	0.175	−0.061	0.114	0.467
ES of P: N	−0.548	−0.329	−0.552	−0.236	−0.011	0.197	0.01	−0.084
Small macroaggregates								
pH	1	0.744[b]	0.653[a]	0.625[a]	0.295	0.272	0.160	0.126
SOC	−0.919[b]	−0.774[b]	−0.634[a]	−0.621[a]	−0.191	0.102	−0.273	−0.081
BG	0.948[b]	0.740[b]	0.590	0.576	0.168	0.140	0.024	0.194
CBH	−0.410	−0.093	−0.136	−0.111	0.151	0.236	0.175	0.070
PhOx	0.944[b]	0.824[b]	0.694[a]	0.559	0.306	0.279	0.182	0.001
Perox	0.889[b]	0.777[b]	0.587	0.582	0.225	0.133	0.102	0.104
AP	−0.842[b]	−0.859[b]	−0.640[a]	−0.589	−0.249	−0.056	−0.081	−0.007
NAG	−0.281	−0.106	−0.064	−0.055	0.090	0.265	0.126	0.331
ES of C: N	−0.178	0.153	−0.143	−0.149	0.083	−0.046	0.004	−0.031
ES of C: P	0.629[a]	0.844[b]	0.515	0.402	0.26	0.165	0.116	−0.078
ES of P: N	−0.740[b]	−0.842[a]	−0.635[a]	−0.52	−0.283	−0.245	−0.172	0.047
Microaggregates								
pH	1	0.372	0.251	0.824[b]	0.425	0.641[a]	0.353	0.659[a]
SOC	−0.770[b]	−0.418	−0.299	−0.711[b]	−0.552	−0.268	−0.555	−0.558
BG	0.801[b]	0.506	0.407	0.728[b]	0.550	0.503	0.358	0.500
CBH	−0.414	−0.504	−0.379	−0.569	−0.526	−0.476	−0.215	−0.273
PhOx	0.847[b]	0.418	0.264	0.775[b]	0.525	0.547	0.294	0.654[a]
Perox	0.899[b]	0.415	0.279	0.829[b]	0.512	0.517	0.227	0.735[b]
AP	−0.797[b]	−0.330	−0.214	−0.657[a]	−0.482	−0.562	−0.126	−0.525
NAG	−0.376	−0.217	−0.123	−0.457	−0.395	−0.360	0.163	−0.375
ES of C: N	−0.193	−0.177	−0.109	−0.147	−0.246	−0.093	−0.278	−0.045
ES of C: P	0.743[b]	0.2	0.161	0.527	0.209	0.296	0.044	0.498
ES of P: N	−0.770[b]	−0.259	−0.193	−0.565	−0.301	−0.344	−0.142	−0.504

SOC, Soil organic carbon; *Total PLFAs*, Total PLFA concentration; *G^+ bacteria*, Gram-positive bacteria; *G^- bacteria*, Gram-negative bacteria; *F: B ratio*, the ratio of fungal biomass to bacterial biomass; *BG*, potential *β*-glucosidase activity; *CBH*, potential cellobiohydrolase activity; *PhOx*, potential phenol oxidase activity; *Perox*, potential peroxidase activity; *AP*, acid phosphomonoesterase potential activity; *NAG*, *N*-acetylglucosaminidase potential activity; *ES*, Enzyme stoichiometry. ES of C: N, C: P and P: N were calculated as potential enzyme activities (BG + CBH + PhOx + Perox)/(BG + CBH + Phox + Perox + NAG), (BG + CBH + PhOx + Perox)/(BG + CBH + PhOx + Perox + AP) and AP/(NAG + AP), respectively.

[a] $P < 0.05$.

[b] $P < 0.01$.

(Al^{3+}) caused by lower soil pH. Notably, Aciego and Brookes (2008) demonstrated that available Al^{3+} concentration escalates dramatically below a pH of 5, surging to 600 mg kg^{-1} soil at pH 4. While some studies, conducted primarily in grassland or agricultural settings with relatively low acidity, report that soil bacterial abundance decreases more significantly than fungal abundance in response to increased acidity (Wang et al., 2021, 2022). However, our findings from a highly acidic subtropical forest soil (pH < 4) shows different results. In such acidic conditions, the extreme acidity may push fungi beyond their acid tolerance limits, increasing their sensitivity. Another explanation for these changes, supported by our experimental data (Fig. S2) and previous research (Liang et al., 2013), is that the SAR treatment significantly decreased fine root biomass, a proxy for root growth. This reduction in fine root biomass indicates a direct impact of prolonged acid rain on the plant's root growth, subsequently decreasing the production of root exudates and ultimately affecting mycorrhizal fungi utilization (Fujii, 2014; Li et al., 2021b; Hu et al., 2022).

Deprotonation of phenolics can elevate redox potential and reduce their solubility in acidic soils, potentially inhibiting enzyme reaction activity (Sinsabaugh, 2010). Consistent with these dynamics, our findings corroborate those reported by Sinsabaugh et al. (2008), indicating a positive correlation between soil pH and the potential activities of BG, PhOx and Perox. In addition, their study identified a weak negative correlation between soil pH and potential CBH activity. Differing from their observations, our results showed that potential CBH activity initially increased with rising soil acidity and then slowed down (Fig. 4). We also detected quadratic relationships between soil pH and potential CBH activity across certain aggregate sizes (Fig. 4), suggesting that CBH maintained relatively high potential activity in low-acid soils compared to other C-degrading potential enzyme activities, but was also suppressed under significantly lower pH levels.

Nutrient limitations, particularly N and P, are commonly the most restrictive factors for forest primary productivity and other biological processes (Vitousek et al., 2010; Zheng et al., 2022). When nutrient demands of forest ecosystems exceed the available supply, there tends to be an increase in the production of extracellular enzymes that facilitate nutrient mineralization (Hu et al., 2022). Thus, potential activities of enzymes such as NAG and AP, which indicate N and P mineralization rates, respectively, serve as key indicators of nutrient limitation in forest ecosystems (Moorhead et al., 2016; Zheng et al., 2022). This study confirms a negative relationship between soil pH and AP activity (Fig. 4), aligning with earlier findings by Sinsabaugh et al. (2008). AP activity was enhanced more than NAG with increasing soil acidity, resulting in a higher enzyme stoichiometry for P/N ratio (Figs. 3 and 4). Given that P limitation is prevalent in tropical and subtropical forests (Huang et al., 2013; Hou et al., 2020), increased soil acidity could have a strong effect on P availability by releasing more increase extractable Al^{3+} (Li and Johnson, 2016; Hu et al., 2022) and facilitating the binding

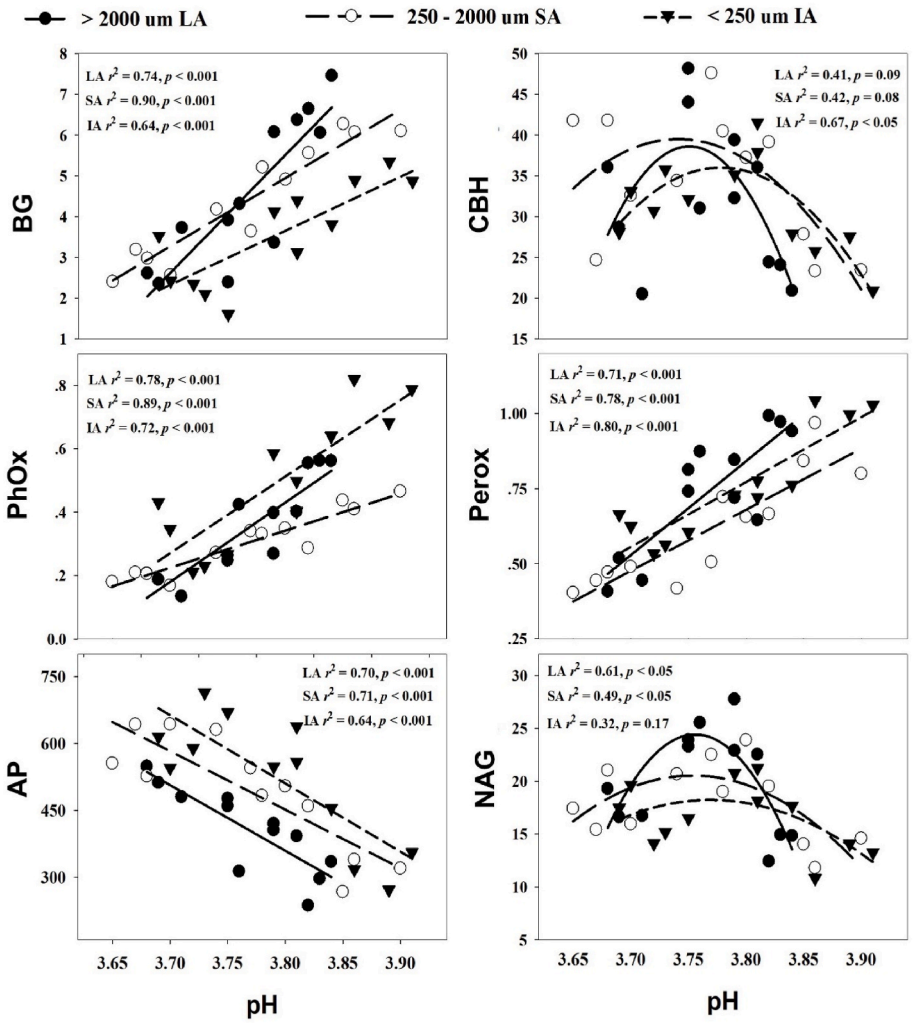

Fig. 4. Relationships between soil pH and the potential enzyme activities among different soil aggregates.
BG, potential *β*-glucosidase activity; *CBH*, potential cellobiohydrolase activity; *PhOx*, potential phenol oxidase activity; *Perox*, potential peroxidase activity; *AP*, potential acid phosphomonoesterase activity; *NAG*, potential *N*-acetylglucosaminidase activity. > 2000 μm, large macroaggregates (LA); *250*-2000 μm, small macroaggregates (SA); < 250 μm, microaggregates (IA).

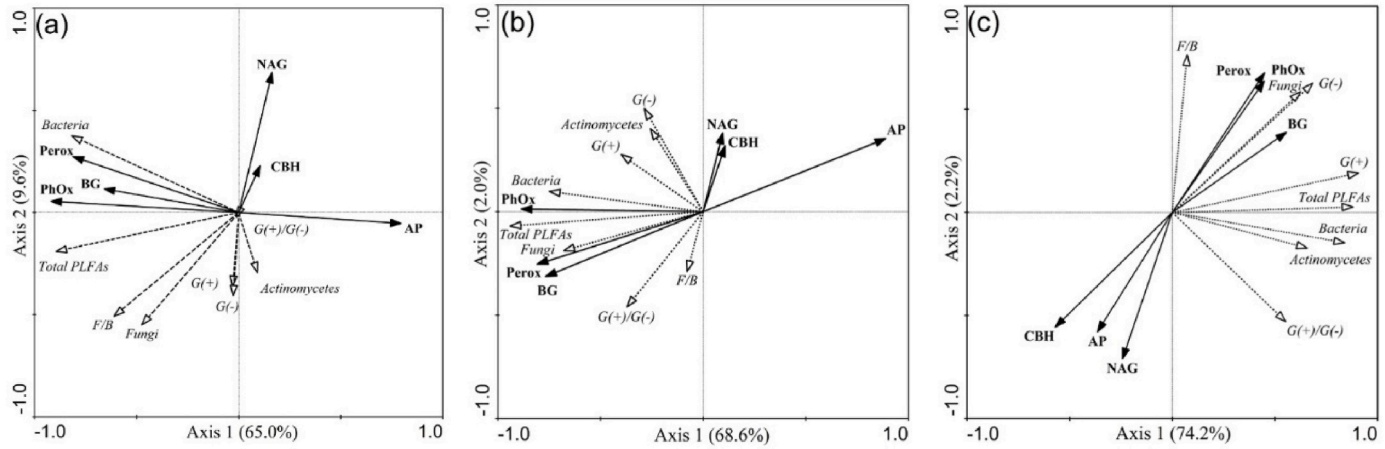

Fig. 5. Redundancy analysis (RDA) of relationship between microbial groups abundance and soil enzyme activities across(a) large macroaggregates (>2000 μm), (b) small macroaggregates (250–2000 μm), and (c) microaggregates (<250 μm). *Total PLFAs*, Total PLFA concentration; *G^+ bacteria*, Gram-positive bacteria; *G^- bacteria*, Gram-negative bacteria; *F:B ratio*, the ratio of fungal biomass to bacterial biomass; *G^+: G^- ratio*, the ratio of Gram-positive bacterial biomass to Gram-negative bacterial biomass; *BG*, potential *β*-glucosidase activity; *CBH*, potential *N*-acetyl-glucosaminidase activity; *PhOx*, potential phenol oxidase activity; *Perox*, potential peroxidase activity; *AP*, potential acid phosphomonoesterase activity; *NAG*, potential *N*-acetyl-glucosaminidase activity.

of phosphate ions with Al^{3+} and ferric ions (Fe^{3+}) (Ma et al., 2021). The reduced P availability could stimulate plant roots and microbial activity to release more AP, aiding in plant P acquisition.

The negative effects of the SAR treatment on microbial abundance did not significantly differ among the three soil aggregate sizes. However, the SAR treatment more significantly limited potential enzyme activities at their optimal positions within these sizes, such as hydrolytic enzymes like BG in macroaggregates and oxidases (PhOx and Perox) in microaggregates. This could be attributed to the dominant roles of specific enzyme activities, which vary according to the compositions of the primary microbial groups within different soil aggregates. Our study also revealed that that the composition of the main microbial groups strongly influenced soil potential enzyme activity, with notable variations across aggregate sizes. Changes in potential enzyme activities under the SAR treatment were predominantly associated with total bacterial FLPAs in macroaggregates, while in microaggregates, they were mainly associated with total fungal PLFAs (Table 2; Fig. 5). This association might be due to the sorption properties of soil microaggregates, which could restrict enzymes access to potential substrates (Totsche et al., 2018). However, the fungal hyphal growth habit allows the enzymes to form "bridges" for potential substrates, thereby expanding their foraging distance (Jastrow et al., 2007; Bahram and Netherway, 2022). The decreased F:B ratio under the SAR treatment, combined with differing controls of bacterial and fungal abundances on enzyme activities across soil aggregate sizes, may thus result in interactive effects on potential enzyme activities in this study, even though no interactive effects were observed on the composition of the main microbial groups.

We also found a significant negative correlation between the potential activities of BG, PhOx, Perox and SOC content across different aggregate sizes (Fig. S3). As the aggregate size decreases, the strength of this negative correlation increases. This trend suggests that the potential enzyme activities have a more pronounced impact on SOC content in smaller aggregates. However, as we mention above, the SAR treatment could suppress potential enzyme activities at their optimal positions, and this suppression likely leads to a more pronounced reduction in enzyme activity in microaggregates compared to larger aggregates. Therefore, the significant reduction in C-degrading potential enzyme activities within microaggregates likely slows the decomposition of organic matter, contributes to greater SOC accumulation in these smaller aggregates. Additionally, the physical structure of microaggregates may provide more effective protection for organic matter, limiting microbial and enzymatic access, and thereby further contributing to SOC stability (Six et al., 2004; Totsche et al., 2018).

The SAR treatment also had a notable impact on soil aggregate distribution, as evidenced by the decreased proportion of large macroaggregates *vs.* an increased in microaggregates (Fig. 1b). This shift in distribution is partly attributed to the stronger inhabitation of C-degrading enzyme activities by the SAR treatment in the micro-than macro-aggregates (Fig. 2), as these potential enzyme activities are crucial for the preservation and transformation of aggregates. The reduced proportion of large macroaggregates under SAR treatment could also result from a combined consequence of diminished plant root response to the highly acidic environment and reduced mycorrhizal fungi activity (Wang et al., 2015b; Hu et al., 2022). Plant root growth, which can serve as a framework for macroaggregate formation via enmeshment (Jastrow et al., 1998; Shi et al., 2021), is adversely affected by lower soil pH, leading to reduced root biomass and inhibited proliferation of fine roots, as demonstrated in studies by Liang et al. (2013) and Yu et al. (2024). Additionally, macroaggregate formation is influenced by the secretion of extracellular polymeric substances (Rilling and Mummey, 2006; Redmile-Gordon et al., 2014). In our current study, the SAR treatment significantly decreased fungal abundance, including arbuscular mycorrhizal fungi (Hu et al., 2021). Unlike macroaggregates, microaggregates primarily consist of primary particles bonded by polyvalent metal cations and enriched with microbial debris, humic materials, or polysaccharide polymers. Consistent with the pH buffering effect observed in acidic soils through the dissolution of Al^{3+} and Fe^{3+}, our investigations, along with prior and subsequent studies (Qiu et al., 2015; Jiang et al., 2016; Chen et al., 2022), demonstrated that SAR treatment contributes to soil acidification, leading to a general reduction in exchangeable calcium ion (Ca^{2+}) and a significant enrichment in soil extractable Al^{3+} and Fe^{3+}. The rise in extractable polyvalent metal cations (Al^{3+} and Fe^{3+}) may explain the observed increase in the proportion of microaggregates at our study site, as documented by Hu et al. (2022). Given the significant changes in mass proportion of aggregates under the SAR treatment, the microbial response to the interaction between acid rain and soil aggregates may be more complex than previously thought. Ultimately, a better understanding of how soil aggregate size distribution mediates microbial responses is essential for improving the ability to model ecosystem responses to environmental changes.

It is worth noting that the effects of adding sulfate and nitrate on microbial activity were not separately considered in the SAR experiment. This is a notable limitation, as both sulfate and nitrate ions have distinct biochemical pathways and can influence soil microbial populations and enzyme activities differently. For example, high nitrate concentrations can lead to eutrophication and subsequent hypoxia, negatively impacting aerobic microbial populations and enzyme activities. Conversely, sulfate can influence sulfur-cycling microorganisms and potentially alter microbial community composition and function. The SAR treatments in this study were created using a 1:1 M ratio of sulfuric acid and nitric acid, which may have masked the individual effects of these ions. Despite this limitation, our study provides valuable insights into the general effects of SAR on soil aggregates and microbial communities. Moreover, the total amounts of sulfate and nitrate added to the plots in this study were relatively small, with only 0.59, 1.25, 3.35 kg ha^{-1} yr^{-1} of sulfate and 1.12, 1.54, 2.91 kg ha^{-1} yr^{-1} of nitrate in the T1, T2, T3 treatments, respectively. Compared to background wet deposition (52.8 kg ha^{-1} yr^{-1} for sulfate and 34.1 kg ha^{-1} yr^{-1} for nitrate), these amounts might have limited impacts on microbial population and activities. However, we recommend that future studies incorporate treatments that isolate the effects of sulfate and nitrate to gain a more comprehensive understanding of how these components of acid rain contribute to changes in soil microbial dynamics and ecosystem functions. Additionally, the use of local lake water, adjusted to different pH levels, introduces another layer of complexity. The lake water could have introduced varying microbial communities into the experimental plots, potentially influencing the results. While we aimed to standardize conditions across treatments, the differing pH levels might have resulted in uneven distribution of these introduced elements. This factor is an inherent part of field experiments involving large-scale environmental manipulations and reflects the natural variability that occurs in such conditions. Future studies should consider the potential impacts of these introduced microbial communities, possibly by including control treatments with sterilized water or accounting for the baseline microbial content of the lake water. This would help in isolating the specific effects of acid rain components and enhance our understanding of their impacts on soil ecosystems.

5. Conclusion

After a decade-long SAR treatment on a subtropical forest in south China, significant shifts were observed in soil aggregate distribution, SOC concentration, microbial community compositions, potential enzymes activities and stoichiometry. Particularly, the SAR treatment significantly affected the abundance of both bacterial and fungal communities, as well as the potential activity of selected C-degrading enzymes. Conversely, the potential enzyme activities for nutrient mineralization and enzyme stoichiometry for P/N ratio were significantly enhanced by the SAR treatment. It also caused a marked shift in soil aggregate distribution, with a tendency for larger aggregates to transform into smaller one. However, those microbial responses varied

among soil aggregate sizes. Microbial communities residing in macroaggregates were more susceptible compared to those in microaggregates, while fungal communities within the microaggregates showed greater sensitivity to long-term acid rain exposure than bacterial communities. Potential activities of PhOx and Perox, which are closely associated with fungal communities, were suppressed by low pH across all three aggregate sizes. Based on the above reasons, our findings indicate that soil acid rain inhibited microbial activities, slowing down the decomposition rate of SOC. This process can enhance the stability of SOC and prolong its retention time in the soil, leading to the preservation and accumulation of SOC. However, this also increases soil nutrient limitation and imbalance, particularly for P in subtropical forests. Given the significant influence of soil aggregate size distribution on microbial responses to environmental changes, further research is necessary to deepen our understanding of these mechanisms and to incorporate them into ecosystem models that can accurately predict soil biogeochemical cycling in the future.

CRediT authorship contribution statement

Jianping Wu: Writing – original draft, Formal analysis. **Xin Xiong:** Writing – review & editing. **Dafeng Hui:** Writing – review & editing. **Huiling Zhang:** Investigation. **Jianling Li:** Methodology. **Zhongbing Chang:** Data curation. **Shuo Zhang:** Investigation. **Yongxian Su:** Visualization. **Xueyan Li:** Formal analysis. **Deqiang Zhang:** Writing – review & editing, Conceptualization. **Qi Deng:** Writing – review & editing.

Declaration of competing interest

The authors declare that they have no known competing financial interests or personal relationships that could have appeared to influence the work reported in this paper.

Data availability

Data will be made available on request.

Acknowledgements

This research was financially supported by the Natural Science Foundation of Guangdong Province, China (grant numbers 2024A1515030190, 2022A1515110403, 2021A1515011471), National Key Research and Development Program of China (grant number 2021YFF0703905), National Natural Science Foundation of China (grant numbers 32371675, 42107269, 32201372), Young Talent Project of GDAS, China (grant number 2023GDASQNRC-0217), GDAS' Project of Science and Technology Development, China (grant number 2024GDASZH-2024010102), Science and Technology Program of Guangzhou, China (grant numbers 2024A04J3347, 2024A04J10004), "Young Top-notch Talent" in Pearl River talent plan of Guangdong Province, China (grant number 2019QN01L763), Guangdong Science and Technology Plan Project, China (grant numbers 2023B1212060046).

Appendix A. Supplementary data

Supplementary data to this article can be found online at https://doi.org/10.1016/j.soilbio.2024.109544.

References

Aciego, P.J.C., Brookes, P.C., 2008. Relationships between soil pH and microbial properties in a UK arable soil. Soil Biology and Biochemistry 40, 1856–1861.
Averill, C., Waring, B., 2018. Nitrogen limitation of decomposition and decay: how can it occur? Global Change Biology 24, 1417–1427.
Awad, Y.M., Lee, S.S., Kim, K., Ok, Y.S., Kuzyakov, Y., 2018. Carbon and nitrogen mineralization and enzyme activities in soil aggregate-size classes: effects of biochar, oyster shells, and polymers. Chemosphere 198, 40–48.
Bahram, M., Netherway, T., 2022. Fungi as mediators linking organisms and ecosystems. FEMS Microbiology Reviews 46, 1–16.
Bai, Z., Ma, Q., Wu, X., Zhang, Y., Yu, W., 2017. Temperature sensitivity of a PLFA-distinguishable microbial community differs between varying and constant temperature regimes. Geoderma 308, 54–59.
Blair, G.J., Lefroy, R.D.B., Lise, L., 1995. Soil carbon fractions based on their degree of oxidation, and the development of a carbon of carbon management index for agricultural systems. Australian Journal of Agricultural Research 46, 1459–1466.
Bossio, D.A., Scow, K.M., 1998. Impacts of carbon and flooding on soil microbial communities, phospholipid fatty acid profiles and substrate utilization patterns. Microbial Ecology 35, 265–278.
Chen, J., Hu, Y., Hall, S.J., Hui, D., Li, J., Chen, G., Sun, L., Zhang, D., Deng, Q., 2022. Increased interactions between iron oxides and organic carbon under acid deposition drive large increases in soil organic carbon in a tropical forest in southern China. Biogeochemistry 158, 287–301.
Chen, X., Li, Z., Liu, M., Jiang, C., Che, Y., 2015. Microbial community and functional diversity associated with different aggregate fractions of a paddy soil fertilized with organic manure and/or NPK fertilizer for 20 years. Journal of Soil and Sediment 15, 292–301.
Chen, X., Shan, X., Shi, Z., Zhang, J., Qin, Z., Xiang, H., Wei, H., 2021. Analysis of the spatio-temporal changes in acid rain and their causes in China (1998-2018). Journal of Resources and Ecology 12, 593–599.
Cheng, J., Zhao, M., Cong, J., Qi, Q., Xiao, Y., Cong, W., Deng, Y., Zhou, J., Zhang, Y., 2020. Soil pH exerts stronger impacts than vegetation type and plant diversity on soil bacterial community composition in subtropical broad-leaved forests. Plant and Soil 450, 273–286.
Dick, W.A., Cheng, L., Wang, P., 2000. Soil acid and alkaline phosphatase activity as pH adjustment indicator. Soil Biology and Biochemistry 32, 1915–1919.
Dorodnikov, M., Blagodatskaya, E., Blagodatsky, S., Marhan, S., Fangmeier, A., Kuzyakov, Y., 2009. Simulation of microbial extracellular enzyme activities by elevated CO_2 depends on soil aggregate size. Global Change Biology 15, 1603–1614.
Du, E., de Vries, W., Liu, X., Fang, J., Galloway, J.N., Jiang, Y., 2015. Spatial boundary of urban 'acid islands' in southern China. Scientific Reports 5, 12625.
Fang, X., Zhou, G., Li, Y., Liu, S., Chu, G., Xu, Z., Liu, J., 2016. Warming effects on biomass and composition of microbial communities and enzyme activities within soil aggregates in subtropical forest. Biology and Fertility of Soils 52, 353–365.
Fanin, N., Moorhead, D., Bertrand, I., 2016. Eco-enzymatic stoichiometry and enzymatic vectors reveal differential C, N, P dynamics in decaying litter along a land-use gradient. Biogeochemistry 129, 21–36.
Fujii, K., 2014. Soil acidification and adaptations of plants and microorganisms in Bornean tropical forests. Ecological Research 29, 371–381.
Garcia-Franco, N., Martinez-Mena, M., Goberna, M., Albaladejo, J., 2015. Changes in soil aggregation and microbial community structure control carbon sequestration after afforestation of semiarid shrublands. Soil Biology and Biochemistry 87, 110–121.
Hou, E., Wen, D., Jiang, L., Luo, X., Kuang, Y., Lu, X., Chen, C., Allen, K.T., He, X., Huang, X., Luo, Y., 2020. Latitudinal patterns of terrestrial phosphorus limitation over the globe. Ecology Letters 24, 1420–2143.
Hu, Y., Chen, G., Chen, J., Sun, L., Li, J., Dou, N., Zhang, D., Deng, Q., 2021. Effects of long-term simulated acid rain on soil microbial community structure in a monsoon evergreen broad-leaved forest in southern China. Chinese Journal of Plant Ecology 45, 298–308 (in Chinese).
Hu, Y., Chen, J., Hui, D., Wang, Y.P., Li, J., Chen, J., Chen, G., Zhu, Y., Zhang, L., Zhang, D., Deng, Q., 2022. Mycorrhizal fungi alleviate acidification-induced phosphorus limitation: evidence from a decade-long field experiment of simulated acid deposition in a tropical forest in south China. Global Change Biology 28, 3605–3619.
Huang, W., Liu, J., Wang, Y.P., Zhou, G., Han, T., Li, Y., 2013. Increasing phosphorus limitation along three successional forests in southern China. Plant and Soil 364, 181–191.
Iyyemperumal, K., Shi, W., 2008. Soil enzyme activities in two forage systems following application of different rates of swine lagoon effluent or ammonium nitrate. Applied Soil Ecology 38, 128–136.
Jastrow, J.D., Amonette, J.E., Bailey, V.L., 2007. Mechanisms controlling soil carbon turnover and their potential application for enhancing carbon sequestration. Climatic Change 80, 5–23.
Jastrow, J.D., Miller, R.M., Lussenhop, J., 1998. Contributions of interacting biological mechanisms of soil aggregate stabilization in restored prairie. Soil Biology and Biochemistry 30, 905–916.
Jiang, J., Wang, Y.P., Yu, M., Li, K., Shao, Y., Yan, J., 2016. Responses of soil buffering capacity to acid treatment in three typical subtropical forests. Science of the Total Environment 563−564, 1068–1077.
Li, W., Johnson, C.E., 2016. Relationships among pH, aluminum solubility and aluminum complexation with organic matter in acid forest soils of the Northeastern United States. Geoderma 271, 234–242.
Li, T., Wang, R., Cai, J., Meng, Y., Wang, Z., Feng, X., Liu, H., Turco, R.F., Jiang, Y., 2021a. Enhanced carbon acquisition and use efficiency alleviate microbial carbon relative to nitrogen limitation under soil acidification. Ecological Processes 10, 32.
Li, Y., Wang, Y., Zhang, W., 2021b. Impact of simulated acid rain on the composition of soil microbial communities and soil respiration in typical subtropical forests in Southwest China. Ecotoxicology and Environmental Safety 215, 112152.
Liang, G., Liu, X., Chen, X., Qiu, Q., Zhang, D., Chu, G., Liu, J., Liu, S., Zhou, G., 2013. Response of soil respiration to acid rain in forests of different maturity in southern China. PLoS One 8, e62207.

Ling, D., Huang, Q., Ouyang, Y., 2010. Impacts of simulated acid rain on soil enzyme activities in a latosol. Ecotoxicology and Environmental Safety 73, 1914–1918.
Liu, X., Fu, Z., Zhang, B., Zhai, L., Meng, M., Zhuang, J., Wang, G.G., Zhang, J., 2018. Effects of sulfuric, nitric, and mixed acid rain on Chinese fir sapling growth in Southern China. Ecotoxicology and Environmental Safety 160, 154–161.
Liu, Z., Shan, X., Wei, H., Zhang, J., Saleem, M., Li, D., Zhang, Y., Ma, R., He, Y., Zhong, J., Liu, Y., 2021. Idiosyncratic responses of microbial communities and carbon utilization to acid rain frequency in the agricultural and forest soils. Global Ecology and Conservation 26, e01429.
Liu, Z., Shi, Z., Wei, H., Zhang, J., 2022. Acid rain reduces soil CO_2 emission and promotes soil organic carbon accumulation in association with decreasing the biomass and biological activity of ecosystems: a meta-analysis. Catena 208, 105714.
Lu, X., Hou, E., Guo, J., Gilliam, F.S., Li, J., Tang, S., 2021. Nitrogen addition stimulates soil aggregation and enhances carbon storage in terrestrial ecosystems of China: a meta-analysis. Global Change Biology 27, 2780–2792.
Lu, X., Mao, Q., Gilliam, F.S., Luo, Y., Mo, J., 2014. Nitrogen deposition contributes to soil acidification in tropical ecosystems. Global Change Biology 20, 3790–3801.
Luo, L., Meng, H., Gu, J., 2017. Microbial extracellular enzymes in biogeochemical cycling of ecosystems. Journal of Environmental Management 197, 539–549.
Ma, J., Ma, Y., Wei, R., Chen, Y., Weng, L., Ouyang, X., Li, Y., 2021. Phosphorus transport in different soil types and the contribution of control factors to phosphorus retardation. Chemosphere 276, 130012.
Meng, C., Tian, D., Zeng, H., Li, Z., Yi, C., Niu, S., 2019. Global soil acidification impacts on belowground processes. Environmental Research Letters 14, 74003.
Moorhead, D., Sinsabaugh, R., Hill, B., Weintraub, M.N., 2016. Vector analysis of ecoenzyme activities reveal constraints on coupled C, N and P dynamics. Soil Biology and Biochemistry 93, 1–7.
Nannipieri, P., Trasar-Cepeda, C., Dick, R.P., 2018. Soil enzyme activity: a brief history and biochemistry as a basis for appropriate interpretations and meta-analysis. Biology and Fertility of Soils 54, 11–19.
Nelson, D.W., Sommers, L.E., 1982. Carbon and organic matter. In: Page Mille, A.L., Keeney, R.H. (Eds.), Methods of Soil Analysis Part 2: Chemical and Microbiological Properties. American Society of Agronomy, Madison, WI, pp. 561–579.
Nie, M., Pendall, E., Bell, C., Wallenstein, M., 2014. Soil aggregate size distribution mediates microbial climate change feedbacks. Soil Biology and Biochemistry 68, 357–365.
Ozlu, E., Arriaga, F.J., 2021. The role of carbon stabilization and minerals on soil aggregation in different ecosystems. Catena 202, 105303.
Parham, J.A., Deng, S.P., 2000. Detection, quantification and characterization of β-glucosaminidase activity in soil. Soil Biology and Biochemistry 32, 1183–1190.
Qiu, Q., Wu, J., Liang, G., Liu, J., Chu, G., Zhou, G., Zhang, D., 2015. Effects of simulated acid rain on soil and soil solution chemistry in a monsoon evergreen broad-leaved forest in southern China. Environmental Monitoring and Assessment 187, 1–13.
Rabbi, S.M.F., Daniel, H., Lockwood, P.V., Macdonald, C., Pereg, L., Tighe, M., Wilson, B. R., Young, I.M., 2016. Physical soil architectural traits are functionally linked to carbon decomposition and bacterial diversity. Scientific Reports 6, 33012.
Redmile-Gordon, M.A., Brookes, P.C., Evershed, R.P., Goulding, K.W.T., Hirsch, P.R., 2014. Measuring the soil-microbial interface: extraction of extracellular polymeric substances (EPS) from soil biofilms. Soil Biology and Biochemistry 72, 163–171.
Rilling, M.C., Mummey, D.L., 2006. Mycorrhizas and soil structure. New Phytologist 171, 41–53.
Rousk, J., Brookes, P.C., Bååth, E., 2009. Contrasting soil pH effects on fungal and bacterial growth suggest functional redundancy in carbon mineralization. Applied and Environmental Microbiology 75, 1589–1596.
Shi, Z., Zhang, J., Xiao, Z., Lu, T., Ren, X., Wei, H., 2021. Effects of acid rain on plant growth: a meta-analysis. Journal of Environmental Management 297, 113213.
Sinsabaugh, R.L., 2010. Phenol oxidase, peroxidase and organic matter dynamics of soil. Soil Biology and Biochemistry 42, 391–404.
Sinsabaugh, R.L., Hill, B.H., Shah, J.J.F., 2009. Ecoenzymatic stoichiometry of microbial organic nutrient acquisition in soil and sediment. Nature 462, 795–798.
Sinsabaugh, R.L., Lauber, C.L., Weintraub, M.N., et al., 2008. Stoichiometry of soil enzyme activity at global scale. Ecology Letter 11, 1252–1264.
Six, J., Frey, S.D., Thiet, R.K., Batten, K.M., 2004. Bacterial and fungal contributions to carbon sequestration in agroecosystems. Soil Science Society of America Journal 70, 555–569.
Streit, K., Hagedorn, F., Hiltbrunner, D., Portmann, M., Saurer, M., Buchmann, N., Wild, B., Richter, A., Wipf, S., Siegwolf, R.T.W., 2014. Soil warming alters microbial substrate use in alpine soils. Global Change Biology 20, 1327–1338.
Totsche, K.U., Amelung, W., Gerzabek, M.H., Guggenberger, G., Klumpp, E., Knief, C., Lehndorff, E., Mikutta, R., Peth, S., Prechtel, A., Ray, N., 2018. Microaggregates in soils. Journal of Plant Nutrition and Soil Science 181, 104–136.
Tabatabai, M.A., 1994. Soil enzymes. In: Mickelson, S.H., Bifham, J.M. (Eds.), Methods of Soil Analysis. Part 2: Microbiological and Biochemical Properties. Soil Science Society of America Inc., Madison, WI, pp. 775–833.
Tian, D., Niu, S., 2015. A global analysis of soil acidification caused by nitrogen addition. Environmental Research Letters 10, 024019.
Tian, J., Dungait, J.A.J., Lu, X., Yang, Y., Hartley, L.P., Zhang, W., Mo, J., Yu, G., Zhou, J., Kuzyakov, Y., 2019. Long-term nitrogen addition modifies microbial composition and functions for slow carbon cycling and increased sequestration in tropical forest soil. Global Change Biology 25, 3267–3281.
Vitousek, P.M., Porder, S., Houlton, B.Z., Chadwick, O.A., 2010. Terrestrial phosphorus limitation: mechanisms, implications, and nitrogen-phosphorus interactions. Ecological Applications 20, 5–15.
Wang, J., Cui, W., Che, Z., Liang, F., Wen, Y., Zhan, M., Dong, X., Jin, W., Dong, Z., Song, H., 2021. Effects of synthetic nitrogen fertilizer and manure on fungal and bacterial contributions to N_2O production along a soil acidity gradient. Science of the Total Environment 753, 142011.
Wang, M., Tang, Y., Anderson, C.W.N., Jeyakumar, P., Yang, J., 2018. Effect of simulated acid rain on fluorine mobility and the bacterial community of phosphogypsum. Environmental Science and Pollution Research 25, 15336–15348.
Wang, R., Dorodnikov, M., Yang, S., Zhang, Y., Filley, T.R., Turco, R.F., Zhang, Y., Xu, Z., Li, H., Jiang, Y., 2015a. Responses of enzymatic activities within soil aggregate to 9-year nitrogen and water addition in a semi-arid grassland. Soil Biology and Biochemistry 81, 159–167.
Wang, R., Dungait, J.A.J., Creamer, C.A., Cai, J., Li, B., Xu, Z., Zhang, Y., Ma, Y., Jiang, Y., 2015b. Carbon and nitrogen dynamics in soil aggregates under long-term nitrogen and water addition in a temperate steppe. Soil Science Society of America Journal 79, 527–535.
Wang, T., Cao, X., Chen, M., Lou, Y., Wang, H., Yang, Q., Pan, H., Zhuge, Y., 2022. Effects of soil acidification on bacterial and fungal communities in the jiaodong peninsula, northern China. Agronomy 12, 927.
Wang, C., Guo, P., Han, G., Feng, X., Zhang, P., Tian, X., 2010. Effect of simulated acid rain on the litter decomposition of *Quercus acutissima* and *Pinus massoniana* in forest soil microcosms and the relationship with soil enzyme activities. Science of The Total Environment 408, 2706–2713.
Wang, Y., Hu, N., Ge, T., Kuzyakov, Y., Wang, Z., Li, Z., Tang, Z., Chen, Y., Wu, C., Lou, Y., 2017. Soil aggregation regulates distributions of carbon, microbial community and enzyme activities after 23-year manure amendment. Applied Soil Ecology 111, 65–72.
Waring, B.G., Weintraub, S.R., Sinsabaugh, R.L., 2014. Ecoenzymatic stoichiometry of microbial nutrient acquisition in tropical soils. Biogeochemistry 117, 101–113.
Wu, J., Deng, Q., Hui, D., Xiong, X., Zhang, H., Zhao, M., Wang, X., Hu, M., Su, Y., Zhang, H., Chu, G., Zhang, D., 2020. Reduced lignin decomposition and enhanced soil organic carbon stability by acid rain: evidence from 13C isotope and 13C NMR analyses. Forests 11, 1191.
Wu, J., Liang, G., Hui, D., Deng, Q., Xiong, X., Qiu, Q., Liu, J., Chu, G., Zhou, G., Zhang, D., 2016. Prolonged acid rain facilitates soil organic carbon accumulation in a mature forest in Southern China. Science of the Total Environment 544, 94–102.
Yu, H., Fan, P., Hou, J., Dang, Q., Cui, D., Xi, B., Tan, W., 2020. Inhibitory effect of microplastics on soil extracellular enzymatic activities by changing soil properties and direct adsorption: an investigation at the aggregate-fraction level. Environmental Pollution 267, 115544.
Yu, M., Wang, Y.P., Deng, Q., Jiang, J., Cao, N., Tang, X., Zhang, D., Yan, J., 2024. Soil acidification enhanced soil carbon sequestration through increased mineral protection. Plant and Soil. https://doi.org/10.1007/s11104-024-06608-8.
Zeng, Y., Cao, Y., Qiao, X., Seyler, B.C., Tang, Y., 2019. Air pollution reduction in China: recent success but great challenge for the future. Science of the Total Environment 663, 329–337.
Zhalnina, K., Dias, R., de Quadros, P.D., Davis-Richardson, A., Camargo, F.A.O., Clark, I. M., McGrath, S.P., Hirsch, P.R., Triplettt, E.W., 2015. Soil pH determines microbial diversity and composition in the park grass experiment. Microbial Ecology 69, 395–406.
Zheng, H., Vesterdal, L., Schmidt, I.K., Rousk, J., 2022. Ecoenzymatic stoichiometry can reflect microbial resource limitation, substrate quality, or both in forest soils. Soil Biology and Biochemistry 167, 108613.